Ignition characteristics of Pt, Ni and Pt–Ni catalysts used for autothermal fuel processing

Ahmet K. Avcı [a], David L. Trimm [b], A. Erhan Aksoylu [a], and Z. İlsen Önsan [a,*]

[a] *Department of Chemical Engineering, Boğaziçi University, Bebek 34342, Istanbul, Turkey*
[b] *School of Chemical Engineering and Industrial Chemistry, University of New South Wales, Sydney 2052, Australia*

Received 15 October 2002; accepted 27 February 2003

Oxidation of propane and *n*-butane over supported Pt, Ni and Pt–Ni catalysts was studied under fuel-rich conditions. Light-off temperatures followed the order of propane > *n*-butane and of Ni > Pt–Ni > Pt and were found to have minimum values at optimal fuel : oxygen ratios over Pt–Ni. The bimetallic Pt–Ni catalyst is likely to involve (i) synergistic interactions between the two metals and (ii) pronounced effect of Pt metal during surface ignition. Differences in oxidation activities of Pt and Pt–Ni catalysts seem to be related to the degree of dispersion of Pt metal. For both hydrocarbons, coke formation was not observed under the conditions employed.

KEY WORDS: *n*-butane; nickel; oxidation; platinum; propane.

1. Introduction

The use of proton exchange membrane fuel cells (PEMFCs) in vehicular applications has significant potential since the environmental and operational benefits they offer are much better than those of conventional technologies [1,2]. Hydrogen is known to be the ultimate fuel for PEMFCs [1,2], but problems related to its availability, distribution and on-board storage remain as serious technical hurdles against the commercial use of fuel cells in vehicles. The integration of fuel cells with compact and efficient fuel processors which convert available hydrocarbon fuels to hydrogen is therefore considered [1–6].

The efficient operation of a fuel processor is mostly based on the successful selection of fuel, fuel conversion mechanism and catalyst combinations. Computer simulations of a number of such combinations have shown that the conversion of LPG—a mixture of propane and *n*-butane—to hydrogen via indirect partial oxidation, i.e. combined total oxidation and steam reforming route, over a supported bimetallic Pt–Ni catalyst is a promising option in terms of optimal hydrogen production [7,8]. It is generally accepted that Pt and Ni are the most preferred metals to be used as oxidation [9,10] and steam reforming [11] catalysts, respectively. The presence of these active metals on the same support facilitates heat transfer between exothermic oxidation and endothermic steam reforming on a microscale, thus allowing advanced heat management and thermally efficient hydrogen production. This situation was verified by Ma and Trimm [12] in autothermal conversion of methane to hydrogen. Therefore, the ultimate goal is to drive the partial oxidation of propane and *n*-butane in the most energetically efficient way, where the bimetallic Pt–Ni catalyst particles are employed as "micro heat exchangers".

The first step in indirect partial oxidation is the initiation of catalytic combustion called surface ignition. Surface ignition is important for the heat management of the fuel processor/fuel cell system. Oxidation of propane over Pt has been widely investigated in all fuel regimes [9,10,13–16] while limited data have been reported for Ni catalysts [9,13]. Combustion of *n*-butane has been studied to a much lesser extent, and reported data are scarce [13,17]. Although reports on the kinetics of methane oxidation [18] and on autothermal methane conversion [12] over the bimetallic Pt–Ni catalyst are available, results associated with C_3–C_4 alkane oxidation do not exist. In this work, ignition characteristics of propane and *n*-butane over the bimetallic Pt–Ni catalyst are studied under conditions pertinent to fuel processor operation in the fuel-rich regime. A number of fuel : oxygen ratios and the individual roles of the active metals, Pt and Ni, are studied through a series of reaction tests for the assessment of catalytic activity and via electron microscopy studies for detailed surface characterization of the catalysts.

2. Experimental

Three catalysts, Pt/δ-Al_2O_3, Ni/δ-Al_2O_3 and Pt–Ni/δ-Al_2O_3, were prepared. γ-Al_2O_3 (Alcoa) was dried at 423 K for 2 h and then calcined at 1173 K for 4 h to

* To whom correspondence should be addressed.
E-mail: onsan@boun.edu.tr

1011-372X/03/0500-0017/0

obtain the thermally stable δ-Al_2O_3 support. BET surface areas were measured using a Micromeritics Flowsorb II 2300 apparatus as 279 m^2/g for γ-Al_2O_3 and 82 m^2/g for δ-Al_2O_3. The monometallic Pt/δ-Al_2O_3 and Ni/δ-Al_2O_3 catalysts were prepared by the incipient-to-wetness impregnation technique using aqueous solutions of $Pt(NH_3)_4(NO_3)_2$ (Aldrich) and $Ni(NO_3)_2{\cdot}6H_2O$ (Merck), respectively. The metal loadings were 0.2 wt% for platinum and 15 wt% for nickel. The resulting slurries, which were formed after ultrasonic mixing of the aqueous solutions and the support (ca. 1 ml solution/g support) under vacuum for 1.5 h, were then dried overnight at 393 K and calcined either at 773 K (PtO/δ-Al_2O_3) or at 873 K (NiO/δ-Al_2O_3) for 4 h. The bimetallic catalyst was prepared through a sequential route in which the Pt solution was impregnated over initially prepared and calcined Ni catalyst. Upon Pt impregnation, the final slurry was then dried at 393 K and re-calcined at 773 K for 4 h. Surface characterization of the catalyst samples was carried out using scanning electron microscopy–backscattered composition imaging (SEM-BCI), energy dispersive X-ray analysis (EDX) and particle size analysis techniques, using a Philips XL30 ESEM-FEG system which has a maximum resolution of 2 nm. In EDX analyses, the minimum detection limit was 50 ppm. Coke formation was examined using the thermogravimetric analysis (TGA) technique with a Mettler-Toledo TGA/SDTA851[e] system.

Reaction tests were conducted in stainless steel tubular down-flow microreactors. In all experiments, 50 mg of fresh catalyst was diluted with 200 mg of inert δ-Al_2O_3. The temperature of the catalyst bed was controlled by a Shimaden FP-21 programmable temperature controller to ± 0.1 K. Prior to reaction tests, the catalysts were pretreated by reduction in 20 ml/min of pure hydrogen flow at 773 K for 4 h. The flow of high-purity feed gases—C_3H_8, n-C_4H_{10}, dry air and N_2—was controlled by Omega 5850 series mass flow controllers. A constant flow of hydrogen used in reduction was maintained using an Aalborg GFC171S series mass flow controller. The reaction temperature was increased at a rate of 1 K/min, starting from an initial temperature ranging between 378 and 463 K to a final temperature ranging between 603 and 678 K, depending on the fuel:oxygen ratio and the catalyst of interest. The hydrocarbon flow was kept at 1 ml/min, dry air (oxidant) and N_2 (balance gas) flow rates were adjusted according to the assigned fuel:oxygen ratio ($0.48 < C_3H_8:O_2 < 2.00$; $0.37 < n$-$C_4H_{10}:O_2 < 2.12$). The total inflow was kept constant at 140 ml/min. High flow rates and catalyst dilution were preferred to eliminate temperature rises and hot-spots that may occur due to the exothermicity of oxidation reactions.

Two gas chromatographs operating in parallel were employed for product analysis. Hydrocarbons and CO_2 were analyzed using a Shimadzu GC-14A gas chromatograph equipped with a Porapak Q column at 363 K and a TCD at 423 K, under 25 ml/min of He carrier. Fixed gases (H_2, O_2, N_2 and CH_4) were analyzed using a Shimadzu GC-8A gas chromatograph equipped with a Molecular Sieve 5A column at 333 K and a TCD at 363 K under 50 ml/min of Ar carrier. Two salt–ice traps were used to protect the Molecular Sieve 5A column from water. Transfer lines of the reactor and analysis systems were kept at 398 K to prevent possible condensation. Blank tests confirmed that the stainless steel reactor, alumina and glass wool were inert under the reaction conditions.

3. Results and discussion

The oxidation of propane and n-butane can be described by the following reactions:

$$C_3H_8 + 5O_2 = 3CO_2 + 4H_2O, \quad \Delta H^{\circ}_{298} = -2044.0\ \text{kJ/mol} \quad (1)$$

$$n\text{-}C_4H_{10} + 6.5O_2 = 4CO_2 + 5H_2O, \quad \Delta H^{\circ}_{298} = -2658.5\ \text{kJ/mol}. \quad (2)$$

The fuel-rich conditions used in this study involve fuel:oxygen ratios ($HC:O_2$) greater than the corresponding stoichiometric values, which are 0.200 for propane and 0.154 for n-butane. Oxygen is the limiting reactant, and hence hydrocarbon conversions are dictated by the amount of oxygen existing in the feed stream. Maximum conversions that can be achieved in reactions (1) and (2) are equal to $1/[5(HC:O_2)] \times 100$ and $1/[(13/2)(HC:O_2)] \times 100$, respectively; 40% is the highest propane conversion and 30.8% is the highest n-butane conversion when a $HC:O_2$ ratio of 0.5 is used. Therefore, the actual conversions obtained in the experiments are normalized using these maximum values to define the "conversion" employed in this study:

$$\text{conversion} = \frac{\text{actual hydrocarbon conversion}}{\text{maximum attainable hydrocarbon conversion}} \times 100. \quad (3)$$

The light-off curves of propane and n-butane oxidation over Pt/δ-Al_2O_3, Ni/δ-Al_2O_3 and Pt–Ni/δ-Al_2O_3, and the corresponding SEM images of the catalysts, are presented in figures 1, 2 and 3, respectively. The fuel:oxygen ratio is kept at 0.48 for propane and 0.37 for n-butane, so that the maximum theoretical conversion that can be achieved is 42%. Thus, the comparison is made for equal maximum conversion levels. The light-off temperatures are defined as the temperature at which 10% conversion is achieved.

The conversion–temperature plots obtained for propane and n-butane oxidation over Pt/δ-Al_2O_3, Ni/δ-Al_2O_3 and Pt–Ni/δ-Al_2O_3 are given in figures 1(a), 2(a) and 3(a), respectively. For all catalysts, it can be seen that n-butane is oxidized earlier than propane, and

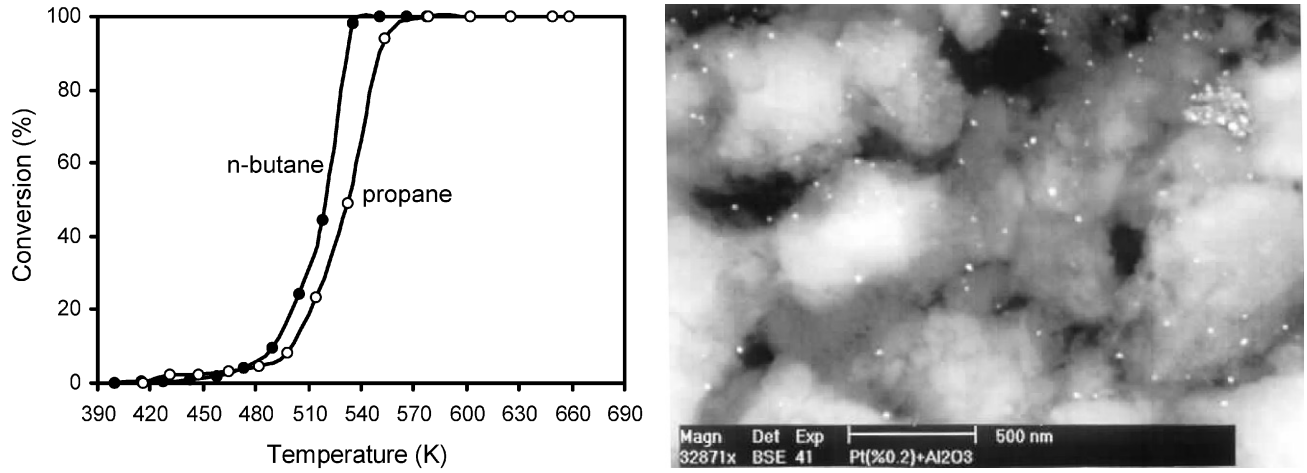

(a) (b)

Figure 1. (a) Conversion–temperature plots for oxidation of propane and *n*-butane over 0.2% Pt/δ-Al_2O_3 catalyst ($C_3:O_2 = 0.48$, n-$C_4:O_2 = 0.37$). (b) SEM-BCI micrograph of the 0.2% Pt/δ-Al_2O_3 catalyst (reduced, fresh sample).

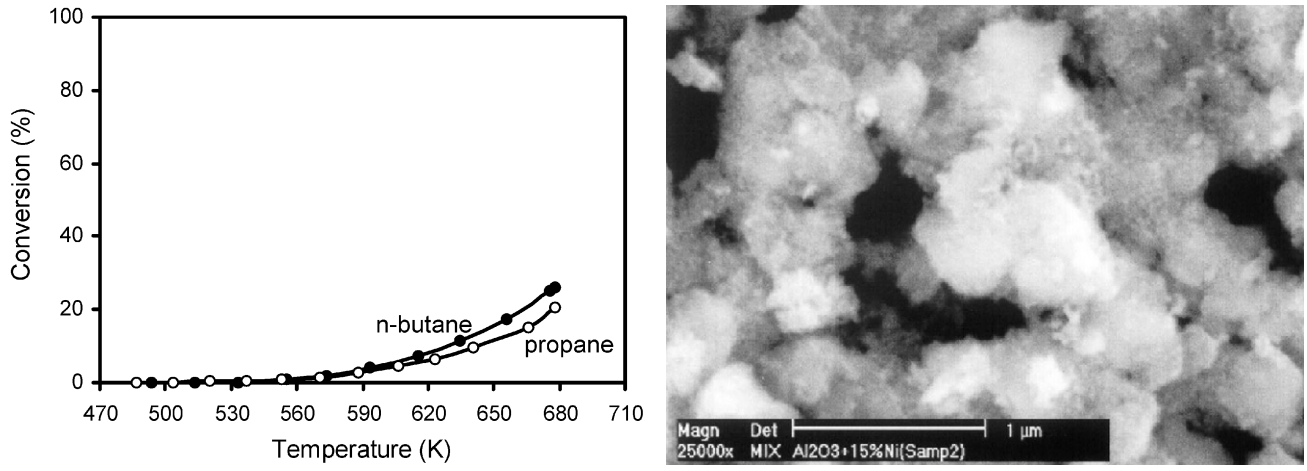

(a) (b)

Figure 2. (a) Conversion–temperature plots for oxidation of propane and *n*-butane over 15% Ni/δ-Al_2O_3 catalyst ($C_3:O_2 = 0.48$, n-$C_4:O_2 = 0.37$). (b) SEM-BCI micrograph of the 15% Ni/δ-Al_2O_3 catalyst (reduced, fresh sample).

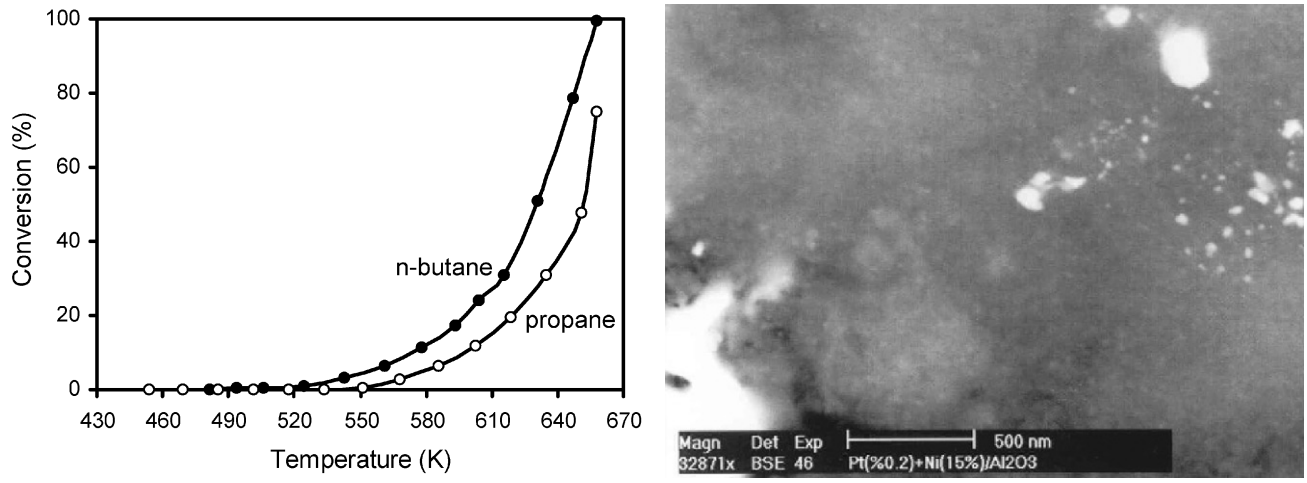

(a) (b)

Figure 3. (a) Conversion–temperature plots for oxidation of propane and *n*-butane over 0.2% Pt–15% Ni/δ-Al_2O_3 catalyst ($C_3:O_2 = 0.48$, n-$C_4:O_2 = 0.37$). (b) SEM-BCI micrograph of the 0.2% Pt–15% Ni/δ-Al_2O_3 catalyst (reduced, fresh sample).

Table 1
Light-off temperatures of propane and *n*-butane

Catalyst	Light-off temperature (K)	
	Propane ($C_3:O_2 = 0.48$)	*n*-Butane (n-$C_4:O_2 = 0.37$)
0.2% Pt/δ-Al_2O_3	501	489
15% Ni/δ-Al_2O_3	643	628
0.2% Pt–15% Ni/δ-Al_2O_3	597	573

the light-off temperatures obtained for *n*-butane are therefore lower (table 1). Since it is generally accepted that the reactivity of alkanes increases with increasing chain length [10,13,19], such a trend is expected. The difference between the light-off temperatures of propane and *n*-butane is not too significant; this difference decreases as the carbon number increases [6].

It is possible to obtain complete "S" curves during temperature-programmed oxidation over the Pt catalyst (figure 1(a)). In the case of Ni, however, the conversion levels achieved are less than 30% within the 390–678 K temperature range (figure 2(a)). This pronounced difference between the oxidation activities of the two catalysts can also be seen quantitatively from the difference of ca. 140 K between the light-off temperatures (table 1), which shows the superior performance of platinum in catalytic combustion [9,19,20]. Although gas-phase oxygen exists in the reaction medium, the Pt sites tend to be in their active metallic state (Pt^0), since the oxides of Pt are known to be unstable. This resistance against transformation into the less active oxide forms makes Pt-based catalysts active in catalytic combustion. High activities of Pt-based catalysts are confirmed also under fuel-lean conditions involving excess oxygen [10,13]. Nickel-based catalysts, on the other hand, are found to exhibit alkane oxidation activities lower than those of platinum (table 1). Although poor oxidation performances have been reported for supported nickel [9,20], Aryafar and Zaera [13] have found nickel to be more active than both platinum and palladium in methane oxidation.

In spite of their poor oxidation features, supported nickel catalysts are known to be effective in driving hydrogen-producing reforming reactions. Therefore, if platinum and nickel metals coexist over the same catalyst, exothermic oxidation and endothermic reforming reactions can run together due to the improved heat transfer on the catalyst surface, which can lead to efficient hydrogen production for fuel cell applications. In the present work, the bimetallic Pt–Ni catalyst was tested for its oxidation characteristics. The oxidation of propane and *n*-butane over the Pt–Ni catalyst is shown in figure 3(a). When compared with the monometallic nickel-catalyzed combustion (figure 2(a)), the light-off temperatures are found to be ca. 50 K lower in the case of the Pt–Ni catalyst (figure 3(a), table 1) even though the amount of platinum is kept as low as 0.2% by weight. However, the monometallic Pt catalyst seems to be much more active than the bimetallic Pt–Ni catalyst in terms of lower light-off temperatures (table 1). The differences between these catalytic activities will be pointed out when the effect of the fuel : oxygen ratio on the ignition behavior of the catalysts is discussed.

The Pt-containing bifunctional catalyst seems to offer some additional features, apart from the better oxidation activity than the monometallic nickel catalyst. In the kinetically controlled regimes of figures 1(a), 2(a) and 3(a), where conversion is below 10% [9], the rate of onset of oxidation (defined as the change in conversion with temperature) over Pt–Ni seems to be greater than those achieved over either of the monometallic catalysts. The SEM image of the Pt–Ni catalyst shown in figure 3(b) indicates that platinum agglomerates, represented by the bright regions, are settled over a nickel environment (gray region in the background) which covers the alumina surface almost completely. However, alloy formation or formation of some other type of new active sites was not detected; SEM-BCI did not indicate any relevant contrast difference. This finding is supported by the EDX results. It can be speculated that the source of this beneficial effect may be the synergistic interactions between Pt and Ni sites. Similar results have also been reported by Opoku-Gyamfi and Adesina [18] who have studied the kinetics of methane oxidation over Pt, NiO and Pt–NiO catalysts. Based on XRD and XPS analyses, they reported that a synergistic interaction existed between Pt and NiO centers rather than the formation of new Pt–Ni active phases. Finally, although SEM studies and literature information provide some ideas about the type of synergy, further detailed studies are required for revealing the interactive characteristics of the bifunctional catalyst.

The fuel : oxygen ratio defines the balance between the amounts of the fuel oxidized/fuel reformed in indirect partial oxidation and has an optimum value that corresponds to maximum hydrogen production [7,8]. The effect of the fuel : oxygen ratio on the light-off temperatures was therefore investigated and is presented in figure 4. The quantitative differences between the light-off temperatures of the different hydrocarbon–catalyst combinations presented in table 1 can clearly be observed for different fuel : oxygen ratios in figure 4. Moreover, these trends indicate several other features of the catalysts. Viewing the abscissa from right to left, it can be seen that, as the amount of oxygen in the feed increases, the light-off temperatures obtained for both propane and *n*-butane decrease to a certain value and then start to increase again in the case of the Pt–Ni catalyst. The formation of minimum light-off temperatures at fuel : oxygen ratios of 1.1 for *n*-butane and 1.8 for propane over the Pt–Ni catalyst can be explained by the possible interaction between two sites. It is very likely that the periphery of Pt agglomerates interacts with the dispersed

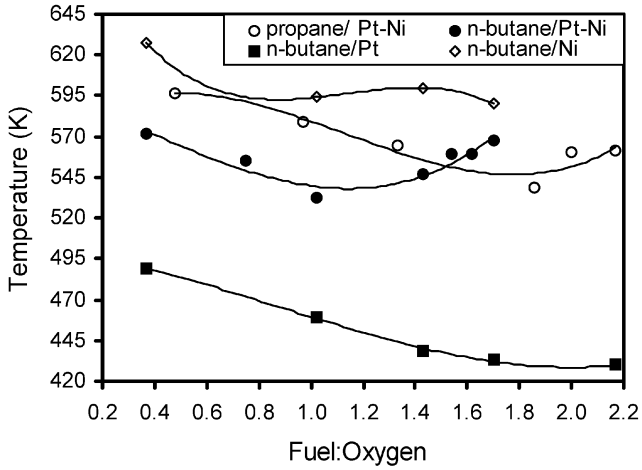

Figure 4. Effect of fuel : oxygen ratio on the light-off temperatures.

Ni environment which modifies the properties of Pt and Ni sites in the Pt-Ni/Al_2O_3 catalyst (figure 3(b)) and leads to increased oxidation activities represented by reduced light-off temperatures at certain fuel : oxygen ratios (figure 4). It can also be speculated that Pt dominates in this interaction which can be supported by the fact that the sticking probability of the C_1–C_4 alkanes on the platinum surface, i.e. the degree of competition with oxygen, increases with hydrocarbon chain length [19]. The inhibiting effect of the hydrocarbon increases and, therefore, that of oxygen decreases in the case of higher alkanes. This phenomenon reported for Pt can also be observed in the case of Pt–Ni, since the minimum fuel : oxygen ratio of *n*-butane is smaller than that of propane, indicating that in the presence of higher quantities of oxygen in the feed the surface ignition of the C_4 alkane is retarded earlier.

In order to understand the roles of each component further, *n*-butane oxidation is studied over monometallic Pt and Ni catalysts under conditions identical with those employed for Pt–Ni (figure 4). At *n*-butane : oxygen ratios less than 1.8, the temperatures obtained over the Pt catalyst decrease steadily as the amount of oxygen fed is decreased, and the rate of temperature decrease on Pt is almost the same as that of Pt–Ni until the minimum point (*n*-butane : oxygen ≈ 1.1) is reached for the latter. On the Pt catalyst, the temperatures remain almost constant beyond a ratio of 1.8, and the increase in the light-off temperatures, which is observed in the Pt–Ni catalyst, is not detected. This difference in behavior can be explained by comparing the SEM images. The SEM image of the monometallic Pt catalyst clearly indicates that platinum particles, represented by the bright specks, are well dispersed over the alumina support which is shown as a white cloud-like structure in the background (figure 1(b)). On the Pt–Ni catalyst, however, the Pt metal is not well dispersed but clustered in certain regions that correspond to bright locations in figure 3(b). These clusters are composed of only Pt, since the EDX studies have shown that the bright regions in figure 3(b) do not include any nickel agglomerates. The difference in platinum dispersion is also confirmed by the particle size analysis; the platinum particles are found to have diameters in the range 10–60 nm and 70–330 nm over Pt/δ-Al_2O_3 and Pt–Ni/δ-Al_2O_3 catalysts, respectively. Therefore, due to the abundance of the active Pt sites over the well-dispersed Pt/δ-Al_2O_3 surface, it can be speculated that oxygen, which has a much higher sticking probability on the Pt surface than that of *n*-butane [19], is the dominant reactant in terms of surface coverage. Hence, the light-off temperatures follow a decreasing pattern even at low quantities of oxygen and the inhibiting effect of *n*-butane cannot be observed as clearly as in the case of the Pt–Ni catalyst. The relatively low number of active Pt sites over the Pt–Ni surface is likely to reduce the surface coverage of oxygen and thus facilitate competition with *n*-butane indicated by the increasing light-off temperatures at ratios greater than 1.1. This argument related to dispersion can probably explain the differences between the light-off temperatures obtained for *n*-butane oxidation over Pt and Pt–Ni catalysts.

The increase in the light-off temperatures obtained for both hydrocarbons over the Pt–Ni catalyst at high fuel : oxygen ratios might also be due to possible carbon formation over Ni which would mask the "operation" of Pt and, therefore, result in lower oxidation activities. In order to investigate the possibility of this scenario, *n*-butane conversion over Pt-Ni/δ-Al_2O_3 was studied in the absence of dry air feed. The reaction temperature was increased from 453 to 623 K at a rate of 1 K/min, with other conditions being kept identical to those given in section 2. The catalyst sample used in the reaction was then analyzed using TGA by heating from 298 to 873 K at a rate of 2 K/min under 25 ml/min flow of pure oxygen. A fresh, reduced catalyst sample was also analyzed using TGA under identical conditions. In both samples, a weight increase of ca. 2% between 423 and 643 K was followed by a minute weight loss of around 0.7% between 673 and 873 K. The identical TGA responses of spent and fresh catalyst samples show that no coke was deposited over the spent catalyst even in the absence of oxygen. Therefore a coking-driven inhibition is unlikely to occur during oxidation at low quantities of oxygen.

The oxidation activity of the Ni/δ-Al_2O_3 catalyst is relatively poor. Although the metal content of the catalyst is as high as 15 wt%, the poor dispersion, i.e. agglomeration of the nickel particles shown in the SEM image as bright regions (figure 2(b)), is likely to contribute to the highest light-off temperatures obtained among the catalysts (table 1). In contrast to the trends obtained for the Pt and Pt–Ni catalysts, the light-off temperatures for *n*-butane oxidation over Ni seem to be less sensitive to the amount of oxygen in the feed (figure 4). Although studies related to Ni-catalyzed

oxidation under fuel-rich conditions are scarce, the active phase of the nickel catalyst during oxidation has been reported to be the relatively stable NiO phase, not the metallic Ni^0 form [21,22]. This may not be adequate to explain the oxygen dependency in alkane oxidation over Ni, but the differences in the trends between the Ni- and the Pt-containing catalysts are likely to support the importance of platinum during oxidation over the Pt–Ni catalyst.

4. Conclusions

The ignition characteristics of propane and *n*-butane over the monometallic 0.2% Pt/δ-Al_2O_3 and 15% Ni/δ-Al_2O_3 catalysts, and over the bimetallic 0.2% Pt–15% Ni/δ-Al_2O_3 catalyst, which offers efficient hydrogen production through facilitating heat transfer between oxidation and reforming reactions, are investigated under fuel-rich conditions. Propane is found to have higher light-off temperatures than *n*-butane over all three catalysts, indicating the elevated paraffin reactivity with increasing chain length. The oxidation activities of the catalysts follow the order of Ni < Pt–Ni < Pt. Synergistic effects due to possible interactions between the periphery of Pt clusters and the Ni environment are likely to facilitate the rate of onset of oxidation and the achievement of minimum light-off temperatures at optimum fuel:oxygen ratios (n-C_4:O_2 = 1.1, C_3:O_2 = 1.8) over Pt–Ni catalysts. Pt metal is likely to dominate in these interactions, since the order of optimum fuel:oxygen ratios are correlated with the order of sticking probabilities of paraffins to the Pt surface. The dispersion of Pt is thought to be responsible for the difference in the responses of Pt and Pt–Ni at high fuel:oxygen ratios and for the differences between the light-off temperatures on the two catalysts. The Ni catalyst shows a non-monotonic response against changes in the amount of oxygen in the feed. Coke formation over the Pt–Ni catalyst, which could drive the mechanism leading to increases in the light-off temperatures at high fuel:oxygen ratios, is not observed. Lower light-off temperatures obtained by the addition of minute quantities of platinum to the steam reforming catalyst (Ni) indicate the possibility of initiating the hydrogen-generating indirect partial oxidation route (total oxidation + steam reforming) with lower energy requirements.

Acknowledgments

The authors would like to thank Ms. Zülal Mısırlı of the Boğaziçi University Advanced Technologies R&D Center for conducting SEM-BCI, EDX and particle size analyses. Financial support was provided by Boaziçi University through projects DPT-97K120640 and DPT-01K120300.

References

[1] T.R. Ralph and G.A. Hards, Chem. Ind. 9 (1998) 337.
[2] W. Vielstich and T. Iwasita, in: *Handbook of Heterogeneous Catalysis*, eds. G. Ertl, H. Knozinger and J. Weitkamp (Wiley, New York, 1997).
[3] G. Hoogers and D. Thompsett, Chem. Ind. 20 (1999) 796.
[4] S. Golunski, Platinum Metals Rev. 42 (1998) 2.
[5] C. Jiang, D.L. Trimm and M.S. Wainwright, Chem. Eng. Technol. 18 (1995) 1.
[6] D.L. Trimm and Z.İ. Önsan, Catal. Rev. Sci. Eng. 43 (2001) 31.
[7] A.K. Avcı, Z.İ. Önsan and D.L. Trimm, Appl. Catal. A 216 (2001) 243.
[8] A.K. Avcı, Z.İ. Önsan and D.L. Trimm, Top. Catal. 22 (2003) 377.
[9] L. Ma, D.L. Trimm and C. Jiang, Appl. Catal. A 138 (1996) 275.
[10] G. Veser, M. Ziauddin and L.D. Schmidt, Catal. Today 47 (1999) 219.
[11] J.R. Rostrup-Nielsen, in: *Catalytic Steam Reforming*, Vol. 5, eds. J.R. Anderson and M. Boudart (Springer, Berlin, 1984) ch. 1.
[12] L. Ma and D.L. Trimm, Appl. Catal. A 138 (1996) 265.
[13] M. Aryafar and F. Zaera, Catal. Lett. 48 (1997) 173.
[14] Y. Yazawa, N. Kagi, S. Komai, A. Satsuma, Y. Murakami and T. Hattori, Catal. Lett. 72 (2001) 157.
[15] H. Wu, L. Liu and S. Yang, Appl. Catal. A 211 (2001) 159.
[16] R. Burch, D.J. Crittle and M.J. Hayes, Catal. Today 47 (1999) 229.
[17] A. Keshavaraja and A.V. Ramaswamy, Appl. Catal. B 8 (1996) L1.
[18] K. Opoku-Gyamfi and A.A. Adesina, Appl. Catal. A 180 (1999) 113.
[19] G. Veser and L.D. Schmidt, AIChE J. 42 (1996) 1077.
[20] K. Tomishige, S. Kanazawa, K. Suzuki, M. Asadullah, M. Sato, K. Ikushima and K. Kunimori, Appl. Catal. A 233 (2002) 35.
[21] D. Dissanayake, M.P. Rosynek, K.C.C. Kharas and J.H. Lunsford, J. Catal. 132 (1991) 117.
[22] L. Ma, PhD Thesis (University of New South Wales, Sydney, 1995).